압전 센서와 액츄에이터를 이용한 단순지지 평판의 능동 진동제어 − I. 이론

Active Vibration Control of a Simply Supported Plate with Piezoelectric Sensors and Actuators − I. Theory

노 용 래*

(Yongrae Roh*)

요 약

압전 센서와 액츄에이터를 이용한 단순지지 평판의 진동제어에 관해 이론적 고찰을 하였다. 적절한 센서, 액츄에이터의 운동방정식을 구한 후 평판의 운동 방정식과 결합해 능동 진동제어 시스템을 구성하였으며, 외력과 제어력의 복합 영향을 고려한 평판의 진동 진폭반응을 해석하였다. 본 방법의 효용성을 보이기 위해 집중 응력과 압전구동기에 의한 모멘트의 두가지 외력에 대한 진동반응을 수치해석 하였으며, 그 결과 압전 센서와 액츄에이터로써 구조물의 외력에 대한 진동반응을 효율적으로 감소시킬 수 있었다. 본 연구에서 고찰된 방법은 임의의 외력 조건과 제어 알고리즘에 적용이 가능하다.

Abstract

Undesired vibratory motion of a simply supported plate is controlled with piezoelectric sensors and actuators. Appropriate dynamic equations of the sensor and actuator are derived and coupled with the dynamic equation of the plate for the construction of an active feedback vibration control system. Analytic solutions are obtained for amplitude response of the plate, reflecting the combined effect of external driving forces and piezoelectric control moments. Numerical examples are presented to illustrate the effectiveness of this approach for two types of external forces, i.e. a concentrated point load and a piezoelectric plate driver. Calculation results show that the sensors and actuators can be efficient tools to mitigate the sensitivity of the structure to external sources of vibration. The method investigated in this work is applicable to arbitrary external loading conditions and control algorithms.

I. Introduction

There are, in general, two categories of techniques available to vibration control specialists: (1) passive method in which the impressed force does work in the damper and (2) active method in which an auxiliary mechanism counteracts the effect of the undesirable force[1]. The control technique has to be efficient and should not increase the size and weight of the components substantially. This paper concerns

* 산업과학기술연구소
접수일자 : 1992. 3. 3.

the active vibration control system that rely in its operation on piezoelectric sensors and actuators. Such systems have been experimentally demonstrated to be effective in suppressing the vibration of simple structural elements like one dimensional rectangular beams[2]. The effectiveness of these systems is consolidated by the light weight, high force and low power consumption capabilities of the sensors and actuators. These features render this method an attracive approach for controlling structural vibration of higher orders.

This paper is concerned with the use of bonded piezoceramic sensors and actuators to actively control vibration in a two dimensional structural dynamic system, a simply supported plate. Deformation of the bonded piezoceramic transducer results in an electrical voltage in the sensor detection unit This signal is conditioned by control circuits adopting various algorithms. The processed signal is used as an input to bonded piezoelectric actuators located at selected positions, and the actuators transmit mechanical energy to the flexible structure. Instantaneous feedback circulation of input signal to controlling energy can reduce overall vibration response of the plate to external forces. A wide selection of feedback algorithm is available in connecting the sensed signal to the actuator[3, 4]. In deciding on the algorithm, one must weigh the ease of implementation of feedback against the desirability of control method. A strategy offering simple implementation is direct feedback control, whereby the control force at a given point depends only on the state at the same point. In this study, therefore, the direct feedback technique is pursued in favor of the simplicity.

This work investigates theoretical aspects of the active vibration control of a simply supported plate and performs analytic derivation of its amplitude response to external forces. The derivation is very general. It can accommodate arbitrary external loading conditions as well as arbitrary number and location of piezoelectric sensor/actuator pairs. Based on the direct feedback control algorithm, numerical examples are presented to illustrate effectiveness of the method for concentrated point loads, piezoelectric plate drivers, and their combination. Calculation results show that the sensors and actuators can effectively reduce the vibration amplitude of the structure responding to external forces. This approach is applicable to any control algorithm.

Ⅱ. Piezoelectric sensors and actuators in a simply supported plate

Ideal sensors or actuators for vibration suppression would be electrically powered, highly efficient, light, and would have a high bandwidth. The high bandwidth requirement allows a designer to construct a closed loop system without regard to sensor and actuator dynamics. Two types of piezoelectric materials are available to choose from, piezoelectric ceramics and piezoelectric polymers, and they each have specific advantages and disadvantages. Both types are electrically powered, are low in mass, and have high bandwidth. Principal advantages of the ceramics are higher electromechanical efficiency, and low voltage operation capability. That of the polymers is the ease of casting the material into an arbitrary surface shape[5]. This study adopts the piezoceramics, **PZT**, as both the sensor and actuator materials.

Piezoelectric material is an inherent electromechanical transducer. An electric field causes it to strain by an amount proportional to the strength of the applied field. The actuator is arranged so that a voltage applied to the electrode surfaces causes the ceramic to expand or contract depending on the polarity of the electric field. Similarly, the bending of the plate stresses the sensor ceramic which in turn produces a voltage to be measured. When the plate is bent by external forces such as initial boundary conditions or harmonic loading, the sensor responds to the applied stress. Above discussion can be summarized in the following two sets of constitutive equations of a piezoelectric material[6].

$$S = s^{De}T + gD_e \qquad E_e = -gT + \beta^T D_e$$
$$S = s^{Ee}T + dE_e \qquad D_e = dT + \varepsilon^T E_e \tag{1}$$

where $\mathbf{S}$ is mechanical strain, $\mathbf{T}$ is mechanical stress, $\mathbf{S}^{De}$ is compliance measured at constant $\mathbf{D}_e$ field, $\mathbf{S}^{Ee}$ is compliance measured at constant $\mathbf{E}_e$ field, $\mathbf{g}$ and $\mathbf{d}$ are piezoelectric stress and strain constants, $\mathbf{D}_e$ is electrical displacement field, $\mathbf{E}_e$ is electric field, ε^T is permittivity measured at constant stress field, and β^T is impermittivity measured at constant stress field. **PZT** has the hexagonal 6mm crystal symmetry after poling. When the crystal **Z** axis is configured to be a poling direction and the other two crystal axes lying on the transversal isotropic basal plane, its piezoelectric stress constant matrix consists of three non-zero independents components as follows:

$$\begin{bmatrix} 0 & 0 & 0 & 0 & g_{15} & 0 \\ 0 & 0 & 0 & g_{24} & 0 & 0 \\ g_{31} & g_{32} & g_{33} & 0 & 0 & 0 \end{bmatrix} \tag{2}$$

where $g_{15}=g_{24}$ and $g_{31}=g_{32}$. The same argument applies to the other set of piezoelectric constants **d**.

Main idea in the use of piezoelectric sensors and actuators for active vibration control is to measure and to cancel the bending moment at specific points of the structure. Figure 1 shows the structural model with the sensor and actuator on. To avoid residual spillover effects, the **PZT** sensor is placed in parallel with the actuator, collinear placement. For the detection purpose, the sensor needs not be large. It is made so small that it is regarded as a point sensor with regard to the vibration modes of interest in this study. The actuator takes the form of a bimorph. The well-known theory of piezoelectric devices says that a bimorph actuator connected in parallel can produce four times more deformation than a unimorph does[7].

Assuming that the stress at the mid-thickness of the **PZT** film is the sensor stress σ_s, the sensor responds to the planar curvature of the plate[8]. From Eq.1, a sensor equation corresponding to Fig. 1-b is

$$\begin{aligned} V_s &= t_s E_s \\ &= t_s g_{31}\sigma_s, \end{aligned} \tag{3}$$

In Eq. 2, $g_{31}=g_{32}$, $g_{36}=0$ and the **PZT** sensor can not respond to surface shear stresses. By linearity,

$$\sigma_s = \sigma_{sx} + \sigma_{sy}, \tag{4}$$

From the plate theory[9],

$$\sigma_{sx} = -Y_s z\left(\frac{\partial^2 w}{\partial x^2} + \nu_s \frac{\partial^2 w}{\partial y^2}\right)\Bigg|_{z=0.5t_p+t_s-t_0}$$

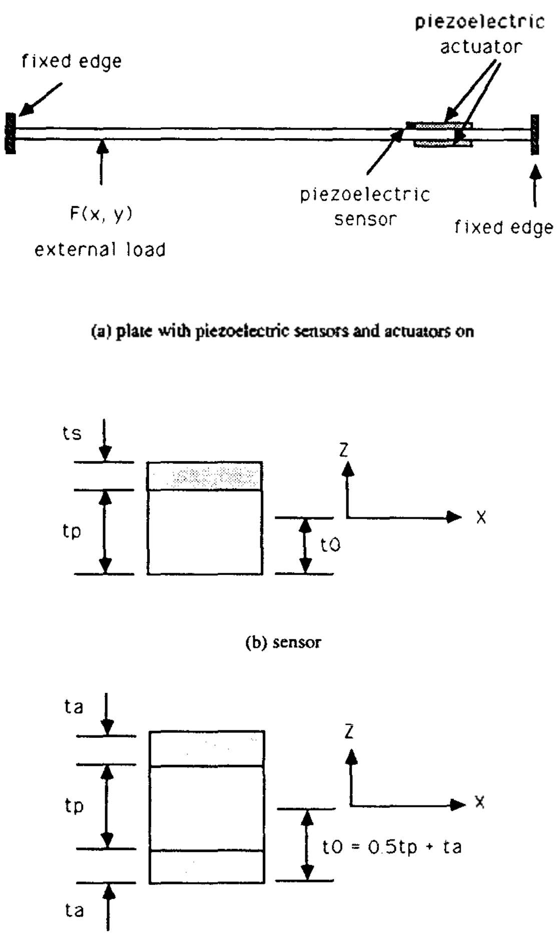

(a) plate with piezoelectric sensors and actuators on

(b) sensor

(c) actuator

Fig. 1. Lateral view of a simply supported plate with piezoelectric sensors and actuators on. t_s is thickness of the sensor, t_a is thickness of the actuator, t_p is thickness of the plate, and t_0 is thickness of the neutral plane

$$= -Y_s s(0.5t_s + t_p - t_0)\left(\frac{\partial^2 w}{\partial x^2} + v_s \frac{\partial^2 w}{\partial y^2}\right)$$

$$\sigma_{sx} = -Y_s s(0.5t_s + t_p - t_0)\left(\frac{\partial^2 w}{\partial y^2} + v_s \frac{\partial^2 w}{\partial x^2}\right) \quad (5)$$

where w is plate displacement, v_s Poisson's ratio of the piezoelectric sensor, and Y_s the effective Young's modulus of the sensor, i.e. plane stress version $Y_s = \frac{Y_s'}{1-v_s^2}$ of the common elastic constant Y_s', respectively. t_0 is the distance of the neutral axis from the bottom of the plate. It is calculated by considering the force balance in the **X** axis of the composite plate as

$$\int_{plate} \sigma_{px}\, dz + \int_{sensor} \sigma_{sx}\, dz = 0 \quad (6)$$

where σpx is the **X** axis stress in the plate and σ_{sx} is the **X** axis stress in the sensor. When the σ_x in Fig. 1 is assumed to vary linearly with the distance z from the neutral axis, Eq. 6 turns out to be

$$\int_{-t_0}^{t_p-t_0} Y_p z\, dz + \int_{t_p-t_0}^{t_s+t_p-t_0} Y_s z\, dz = 0 \quad (7)$$

which yields

$$t_0 = \frac{Y_p t_p^2 + Y_s t_s^2 + 2Y_s t_p t_s}{2(Y_p t_p + Y_s t_s)} \quad (8)$$

where Y_p is the effective Young's modulus of the plate. Therefore when the Eqs. 3, 4, and 5 are combined together, the voltage V_s produced by the **PZT** sensor is

$$V_s = t_s g_{31} Y_s(0.5t_s + t_p - t_0)(1+v_s^2)\left(\frac{\partial^2 w}{\partial x^2} + \frac{\partial^2 w}{\partial y^2}\right) \quad (9)$$

This equation reveals the fact that the measurement is related to the bending strain of the plate which is a generalized displacement.

The bending moment applied by the actuator is determined by integrating the stress produced. The magnitude of the applied moment is found to be proportional to the product of the effective Young's Modulus and piezoelectric strain constant, d_{31} Y_a, the distance from the neutral axis of the plate, and the applied voltage V_a. The actuator equation corresponding to Fig. 1-c is derived as follows.

$$\begin{aligned}
m_{ax} &= \int_{-t_s-0.5t_p}^{t_s+0.5t_p} \sigma_{ax} z\, dz \\
&= \int_{-t_a-0.5t_p}^{-0.5t_p} \sigma_{ax} z\, dz + \int_{0.5t_p}^{0.5t_p+t_a} \sigma_{ax} z\, dz \\
&= \int_{-t_a-0.5t_p}^{-0.5t_p} -Y_a d_{31} E_a z\, dz + \int_{0.5t_p}^{0.5t_p+t_a} Y_a d_{31} E_a z\, dz \\
&= Y_a d_{31}(t_a+t_p)t_a E_a \\
&= Y_a d_{31}(t_a+t_p)V_a \\
&= m_a.
\end{aligned} \quad (10)$$

In a similar manner,

$$m_{ay} = m_a = Y_a d_{31}(t_a+t_p)V_a. \quad (11)$$

where Y_a is the effective Young's modulus of the **PZT** actuator. For sensors, as noted in Eq.9, the PZT with a higher value of g_{31} is preferred, and for actuators, the **PZT** with a higher value of d_{31} is preferred. Unfortunately the **PZT** of high g_{31} does not coincide to be that of high d_{31}. If the same **PZT** meterial is used as both the sensors and actuators, Y_a will be equal to Y_s.

Ⅲ. Theoretical basis for the active vibration contro

The piezoelectric sensor and actuator pairs are placed on a simply supported plate. The sensor detects the current state of the plate when the plate is exposed to external loading conditions. After processed by a control unit, the sensor signal drives the actuator, and the control moment acts as an additional forcing term to the plate. In this investigation, first, the general equation of motion of the plate is analyzed to obtain its vibration response at the sensor location. Once it is found, actuator moment is determined by means of the sensor/actuator functions derived in the previous section. Secondly, the moment is coupled with the initial external forces. Solution of the modified equation of motion will disclose the controlled vibration response of the plate reflecting coupled effect of the external driving forces and piezoelectric control moment.

Figure 2 shows the structural model under investigation. Plate dimension is **a**×**b**×t_p(width×

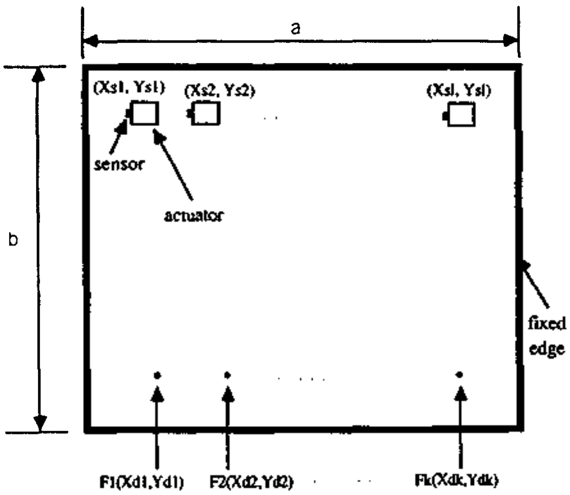

Fig 2. Upper view of the simply supported plate with multiple sensors and actuators on

length×thickness). On top of the plate, κ different inital driving forces $\mathbf{F}(x_d, y_d)$are simultaneously loaded, and induced vibration is controlled by l different piezoelectric sensor/actuator pairs. Governing equation of motion of a simply supported rectangular plate is

$$D\nabla^4 w + \rho \ddot{w} = \sum_{j=1}^{k} F_j(x_{dj}, y_{dj}) \qquad (12)$$

where D is the flexural rigidity YI, I is the second moment of inertia, ρ is the planar density of the plate. When time harmonic terms are omitted for brevity, the plate response is given for an arbitrary initial external force as

$$w(x, y) = \sum_{m=1}^{\infty}\sum_{n=1}^{\infty} \alpha_{mn}\phi_{mn}(x, y) \qquad (13)$$

where α_{mn} is a plate response modal amplitude and is dependent on source locations and source types. For this plate, the eigenfunctions are

$$\phi_{mn}(x, y) = \sin\left(\frac{m\pi x}{a}\right)\sin\left(\frac{n\pi y}{b}\right) \qquad (14)$$

The homogeneous version of Eq. 12 takes the form of a Sturm-Liouville system and the characteristic functions satisfy the following orthogonality conditions.

$$\int_0^b\int_0^a \phi_{mn}\phi_{m'n'}\,dx\,dy = \frac{ab}{4} \qquad \text{if } m = m',\ n = n'$$
$$(15)$$
$$\int_0^b\int_0^a \phi_{mn}\phi_{m'n'}\,dx\,dy = 0 \qquad \text{if } m \neq m',\ n \neq n'$$

The effect of the κ external forces can be regarded as linear superposition of those of individual forces. When Eq. 13 is substituted into Eq. 12, the governing equation for the jth external driving force $F_j(x_{dj}, y_{dj})$becomes

$$\sum_{m=1}^{\infty}\sum_{n=1}^{\infty}(\omega_{mn}^2 - \omega^2)\,\alpha_{mn}^j\phi_{mn} = F_j(x_{dj}, y_{dj}) \qquad (16)$$

where ω_{mn} is the resonant frequency of the plate and is given as

$$\omega_{mn}^2 = \frac{\pi^4 D}{\rho}\left(\frac{m^2}{a^2} + \frac{n^2}{b^2}\right)^2 \qquad (17)$$

where ρ is the planar density of the plate. The plate modal amplitude α_{mn}^j is determined by utilizing the orthogonality of the response eigenfunctions as below.

$$\alpha_{mn}^j = \frac{4}{\rho\, ab\,(\omega_{mn}^2 - \omega^2)}\int_{-\infty}^{\infty}\int_{-\infty}^{\infty} F(x_{dj}, y_{dj})\phi_{mn}(x, y)\,dx\,dy \qquad (18)$$

When Eq. 18 is summed up for all the κ driving forces $F(x_d, y_d)$and plugged into Eq. 13, w(x, y) give the total vibration amplitude response of the plate. L different sensors are placed on top of the plate to detect the vibration, and the plate amplitude at the ith sensor location (x_{si}, y_{si}) is given as

$$w_i(x_{si}, y_{si}) = \sum_{m=1}^{\infty}\sum_{n=1}^{\infty}\left[\sum_{j=1}^{k}\alpha_{mn}^j\right]\phi_{mn}(x_{si}, y_{si}) \qquad (19)$$

This is substituted into Eq. 9 and the induced voltage at the ith sensor is determined by

$$V_{si} = t_s g_{31} Y_s (0.5t_s + t_p - t_{si})(1 + \nu_s^2)\nabla^2 w_i(x_{si}, y_{si}) \qquad (20)$$

The measured signal is conditioned by the control unit. The conditioning includes filtering, phase shifting and amplifying. By virtue of the actuator, the modified signal is reinput to the structure in the form of bending moment counterbalancing the original moment of the plate. The sensor and actuator blocks exhibit no dynamics because their bandwidth is far beyond that of the control loop. After passing through control circuits, the electrical potential applied to the *i*th piezoelectric actuator corresponding to the *i*th sensor becomes

$$V_{ai} = G_i V_{si} \tag{21}$$

where G_i is the amplifier gain of the *i*th controller. Actually the G_i denotes the transfer funciton of the *i*th control unit relating input voltage V_{si} to output voltage V_{ai}. All the effect of control algorithm is reflected in this G_i. It does not have to be a positive real number. Control processing speed is assumed to be so high that the controller's time delay is considered negligible. Control moment applied by the actuator is from Eq. 10,

$$\begin{aligned} m_a &= m_{xai} = m_{yai} \\ &= Y_a d_{31}(t_a+t_p)\, V_{ai} \\ &= Y_a d_{31}(t_a t_p)\, G_i \{ t_s g_{31} Y_s\, (0.5\, t_s+t_p-t_0) \\ &\quad (1+v_s^2) \nabla^2 w_i(x_{si}, y_{si}) \} \\ &= S\, G_i \nabla^2 w_i(x_{si}, y_{si}) \end{aligned} \tag{22}$$

where

$$S = Y_a d_{31}(t_a t_p) \{ t_a g_{31} Y_s\, (0.5\, t_s+t_p-t_0)\, (1+v_s^2) \}$$

This is for the actuator having unit length and unit width. For a general rectangulat actuator having arbitrary length and width, Eq. 22 changes to

$$\begin{aligned} M_{xai} &= m_{xai} [h(x-x_{ai1}) - h(x-x_{ai2})] \\ &\quad [h(y-y_{ai1}) - h(y-y_{ai2})] \\ M_{yai} &= m_{yai} [h(x-x_{ai1}) - h(x-x_{ai2})] \\ &\quad [h(y-y_{ai1}) - h(y-y_{ai2})] \end{aligned} \tag{23}$$

where **h** is the Heavyside step function, and the *i*th actuator spans from x_{ai1} to x_{ai2} and from y_{ai1} to y_{ai2}. These control moments act on the plate as additional forcing functions in Eq. 12. Therefore, when the effect of all the *l* actuators is added up, the final equation of motion becomes

$$D\nabla^4 w + \rho \ddot{w} = \sum_{j=1}^{k} F_j(x_{dj}, y_{dj}) + \sum_{i=1}^{l} \left(\frac{\partial^2 M_{xai}}{\partial x^2} + \frac{\partial^2 M_{yai}}{\partial y^2} \right) \tag{24}$$

When Eq. 23 is plugged into Eq. 24, the final equation of motion looks like

$$\begin{aligned} D\nabla^4 w + \rho \ddot{w} &= \sum_{j=1}^{k} F_j(x_{dj}, y_{dj}) \\ &\quad - \sum_{i=1}^{l} \{ m_{xi}{}^* [\delta'(x-x_{ai1}) - \delta'(x-x_{ai2})]^* \\ &\quad [h(y-y_{ai1}) - h(y-y_{ai2})] + m_{yi}{}^* \\ &\quad [h(x-x_{ai1}) - h(x-x_{ai2})]^* [\delta'(y-y_{ai1}) \\ &\quad - \delta'(y-y_{ai2})] \} \end{aligned} \tag{25}$$

where δ' is a doublet. The corresponding final response of the plate is defined as

$$w(x, y) = \sum_{m=1}^{r} \sum_{n=1}^{r} \beta_{mn} \phi_{mn}(x, y) \tag{26}$$

where β_{mn} is a plate total response modal amplitude.

The total response consists of two groups, each one due to (1) initial external load F, and (2) controlling moments M_{xa} and M_{ya}, respectively. In this analysis, respective response to each group of forcing functions is calculated by utilizing the orthogonality of the eigenfunctions, and the final amplitude response will be determined by summing up the individual responses based on the principle of linear superposition.

(1) *first forcing function group*—*this term is* the initial external load $F(x_d, y_d)$ and the response is the same as the Eq. 18.

$$\beta^1_{mn} = \sum_{j=1}^{k} \alpha^j_{mn} \tag{27}$$

(2) second forcing function group-the response to this group is found, in a similar manner, as

$$\beta^2_{mn} = \frac{-4}{\rho\, ab\,(\omega^2_{mn}-\omega^2_a)} * \left(\frac{\frac{m^2\pi^2}{a^2}+\frac{n^2\pi^2}{b^2}}{\frac{m\pi}{a}\ \frac{n\pi}{b}} \right)$$
$$* \sum_{i=1}^{L} \{ m_{ai} * [\cos(\frac{m\pi}{a} x_{ai1}) - \cos(\frac{m\pi}{a} x_{ai2})]$$
$$[\cos(\frac{n\pi}{b} y_{ai1}) - \cos(\frac{n\pi}{b} y_{ai2})] \quad (28)$$

where ω_a is the frequency of the signal applied by the actuator. ω_a can be the same as the initial external loading frequency ω in Eq. 18. However, if filtering of the sensor signal is included in the control circuit, which is the usual case, ω_a may be different from the external loading frequency. When these are combined together, the final controlled amplitude response of the plate is

$$w(x, y) = \sum_{m=1}^{r} \sum_{n=1}^{r} \beta_{mn}\, \phi_{mn}(x, y)$$
$$= \sum_{m=1}^{r} \sum_{n=1}^{r} (\beta^1_{mn} + \beta^2_{mn})\, \phi_{mn}(x, y) \quad (29)$$

Equation 29 is a very general equation for feedback vibration control of a simply supported plate without any restrictions. The equation shows the coupled effect of initial driving forces and piezoelectric control moment on overall amplitude response of the plate. The whole purpose of this study is to reduce the vibration amplitude of the plate in response to external forces. For measurement of the efficiency of the control method, the absolute value of the amplitude over all the plate surface is calculated.

$$\int_0^b \int_0^a \phi \sum \sum \beta_{mn}\, \phi_{mn}(x, y)\,]^2\, dx\, dy \quad (30)$$

Equation 30 can be analyzed in many different ways. For constant external forces, it is a function of input source locations, sensor locations, actuator locations and sizes, and amplifier gains. Once the magnitude and location of the initial external force is known, by the help of multivariate minimization techniques such as Downhill Simplex Method due to Nelder and Maed [10], all of the above variables can be optimized to get the minimum value of A. Certain criteria for the selection of the sensor and actuator locations like the preference of anti-nodal points will reduce the number of variables to be minimized This sort of analysis will be presented in the author's consecutive paper. But in the case of random distribution of initial forces, which is a rather common case explaining why it is called "noise", the location of the external forces changes from time to time. However, the sensor and actuator can not alter their positions tracking the change of disturbance sites. Hence, for a general external force when the sensors and actuators are fixed at certain predetermined places, the amplifier gain is the only remaining controllable variable.

Equation 30 can be written in terms of the gain G_i in a simplified notation as follows.

$$A = [\Gamma + \sum_{i=1}^{L} G_i\, \Psi_i]^2 \quad (31)$$

This equation is minimized by use of the above mentioned Downhill Simplex optimization algorithm. Here, the minimized value of G_i is not the same as the modal control gain in the optimal control technique. Each G_i corresponds the amplifier gain of each controller with the specific control algorithm. Once the optimal amplifier gain G_i is determined from Eq. 31, the result is substituted into Eq. 29. This concludes our derivation of the response function, and it gives the optimally controlled vibration amplitude of the plate in response to external forces.

IV. Numerical Analysis

Use of the Eq. 29 is exemplified for two types of external forces, concentrated point loads and **PZT** plate drivers. The plate is made of aluminium. Table 1 shows material properties and dimensions of the plate as well as the **PZT** sensors and actuators. This study focuses on the general analysis of actively controlled vibration response of a simply supported plate to external forces. Development of new control algorithm is not the target of current investigation. Hence, of a great variety of control algorithm, direct proportional feedback control method is adopted due to its simplicity and ease of implementation. Further, it is assumed that just one controller is used for the vibration suppression. It means that all the sensor and actuator pairs share the same controller and we have just one amplifier gain to be evaluated. In this case, Eq. 31 reduces to a simple quadratic equation of G. The value of G minimizing A is easily calculated as the root of the first derivative of A with respect to G. In the calculation, the summation index m and n are included up to 5, respectively, which is accurate enough. Numerical results are obtained for four different lowest modes, (1, 1), (1, 2), (2, 2), and (1, 3).

Table 1. Material specifications of the plate and PZT sensor/ actuator

plate length	36.0 cm
plate width	36.0 cm
plate thickness	0.05 cm
plate density	$2.7\ g/cm^3$
plate Young's modulus	$73\ GN/m^2$
plate Poisson's ratio	0.31
PZT actuator length	1.0 cm
PZT actuator width	1.0 cm
PZT sensor and actuator thickness	0.02 cm
PZT density	$7.5\ g/cm^2$
PZT Young's modulus	$139\ GN/m^2$
PZT d_{31}	$123\times10^{-12}\ m/V$
PZT g_{31}	$-11.9\times10^{-3}\ Vm/N$
PZT poisson's ratio	0.31

4.1. Point Loads

The initial force function $F_d(x_d, y_d)$ in Eq. 12 is κ concentrated point loads P_i located at (x_{di}, y_{di}). The equation changes to

$$D\nabla^4 w + \rho \ddot{w} = \sum_{i=1}^{k} P_i\, \delta(x-y_{di})\, \delta(y-y_{di}) \qquad (32)$$

The plate response modal amplitude α^{j}_{mn} in Eq. 18 is determined by utilizing the orthogonality properties of the response eigenfunctions as

$$\alpha^{j}_{mn} = \frac{4p}{\rho\, ab(\omega^2_{mn} - \omega^2)} \sin\left(\frac{m\pi x_{dj}}{a}\right) \sin\left(\frac{n\pi y_{dj}}{b}\right) \qquad (33)$$

This equation is substituted into Eq. 29 and the final amplitude response to various types of external point sources is calculated. Three different combinations of point loads and PZT sensor/actuator pairs are considered to show the generality of the derivation.

4.1.1. one point load and one PZT sensor/actuator pair

In Fig. 2, one 10N concentrated load is applied at (0.27, 0.27) and the center of one PZT sensor/actuator pair is placed at (0.9, 0.9). The point source frequency is adjusted at the first resonance of the plate. Without the actuator, the response is as shown in Fig. 3. It shows the (1, 1) mode shape and has the maximum amplitude of 6 cm. When the control moment is coupled with the point load, the amplitude response changes to Fig. 4. Maximum amplitude reduces to 0.8 cm. Figure 5 is the magnified view of the controlled vibration amplitude, which allows a clear view of the actuator effect. By means of oppositely sensed control moment, the peak at the source location decreases and a new downhill peak is generated at the actuator location. Figure 6 shows relative amplitude suppression ratios in terms of the decibel unit. There is a deep valley around the actuator. The valley corresponds to the points where the amplitude becomes almost zero after control. Maximum amplitude reduction is -90.7 dB at the valley and average reduction all over the plate surface is -24.7 dB. When the source frequency is tuned at the (1, 2) resonance of the plate, amplitude response without the controller is as in Fig. 7, and that with the controller is as in Fig. 8. Here also, at least around the actuator, the curvature of the plate changes its sign after control Maximum amplitude suppression is -75.4 dB and average suppression is -23.1 dB. When the source frequency is adjusted at the (2, 2) and (1, 3) resonance of the plate, similar results are obtained as in Figs. 9, 10 and Figs, 11, 12, respectively. Maximum amplitude reductions are -70.5 dB and -68.4 dB for each case, and occurs around the actuator position Average reductions are -28.0 dB and -15.0 dB, respect-

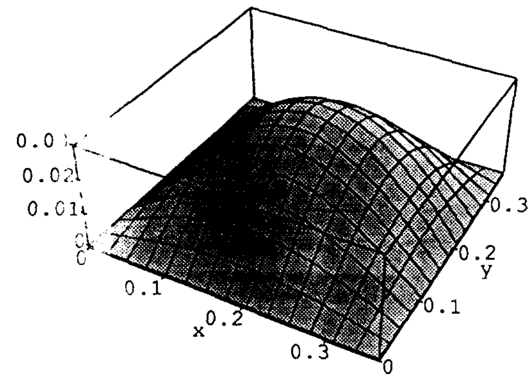

Fig 3. Vibration amplitude response of the simply supported plate exposed to one point load tuned at(1,1) mode without any control effect

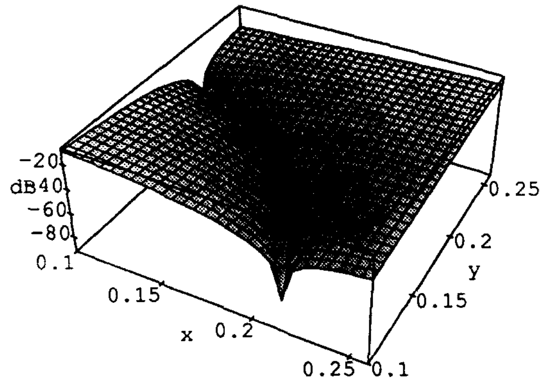

Fig 6. Vibration amplitude reduction after the active vibration control when the plate is exposed to one point load tuned at(1,1) mode

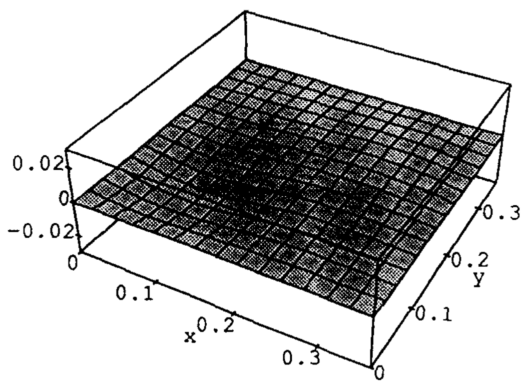

Fig 4. Vibration amplitude response of the simply supported plate exposed to one point load tuned at(1,1) mode and one **PZT** sensor / actuator pair

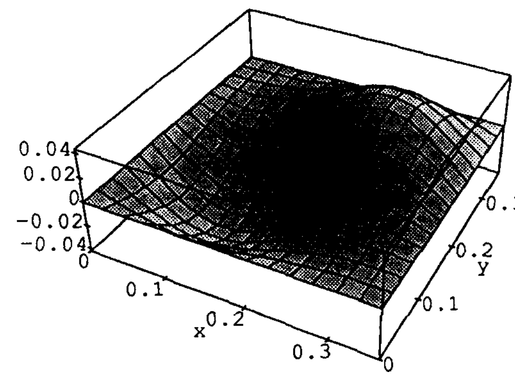

Fig 7. Vibration amplitude response of the simply supported plate exposed to one point load tuned at(1,2) mode without any control effect

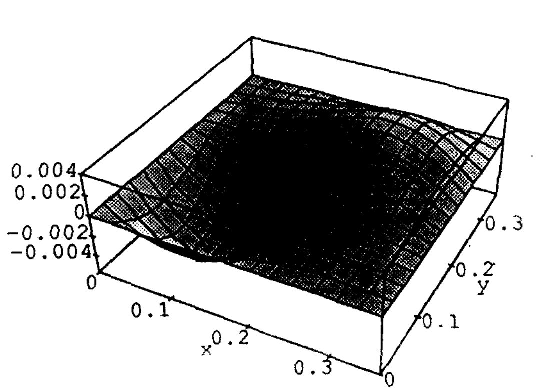

Fig 5. Magnified view of vibration amplitude response of the plate exposed to one point tuned at(1,1) mode and one **PZT** sensor / actuator pair

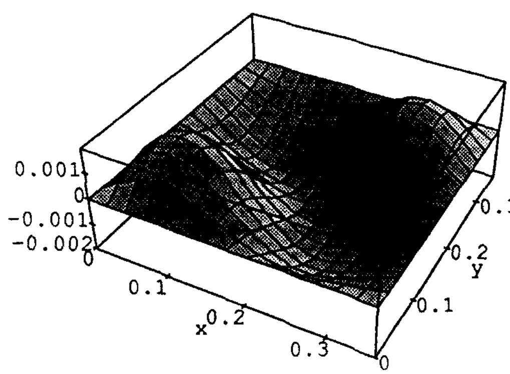

Fig 8. Vibration amplitude response of the simply supported plate exposed to one point load tuned at(1,2) mode and one **PZT** sensor / actuator pair

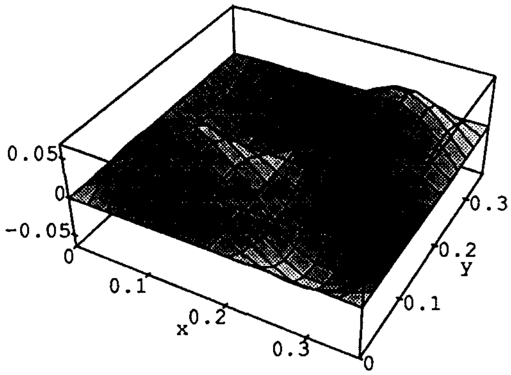

Fig 9. Vibration amplitude response of the simply supported plate exposed to one point load tuned at(2,2) mode without any control effect

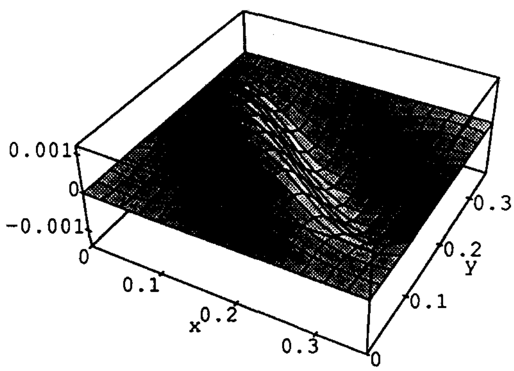

Fig 10. Vibration amplitude response of the simply supported plate exposed to one point load tuned at(2,2) mode and one **PZT** sensor /actuator pair

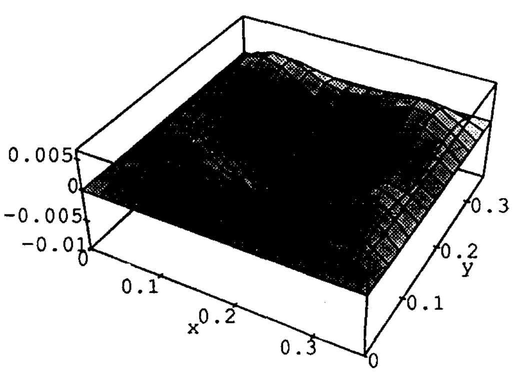

Fig 11. Vibration amplitude response of the simply supported plate exposed to one point load tuned at(1,3) mode whithout any control effect

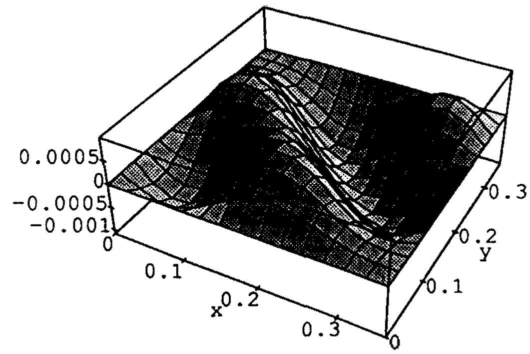

Fig 12. Vibration amplitude response of the simply supported plate exposed to one point load tuned at(1,3) mode and one **PZT** sensor /actuator pair

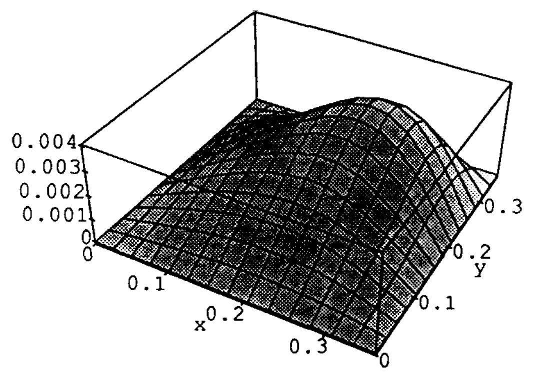

Fig 13. Vibration amplitude response of the simply supported plate exposed to one point load tuned at 30 rad. /sec. without any control effect.

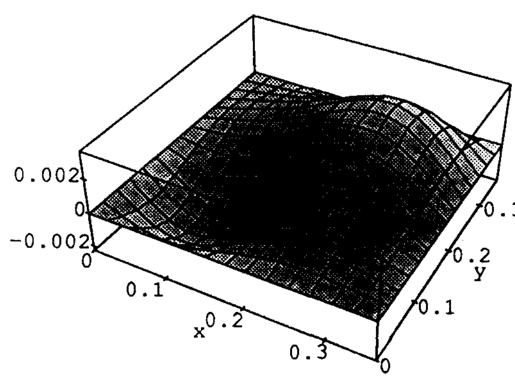

Fig 14. Vibration amplitude response of the simply supported plate exposed to one point load tuned at 30 rad. /ses. and one **PZT** sensor /actuator pair

ively. Higher modes of vibration can be analyzed in the same fashion.

As seen in the results, the control efficiency of the sensor/actuator pair varies for each mode. It is because the fixed sensor/actuator position is not always good for all the modes of vibration. Main idea employed in the analysis is to control the vibration by measuring and cancelling the bending moment at a specific point of the structure. The optimal location of the sensor and actuator for each mode should be therefore where the specific mode's maximum bending moment occurs when the plate is loaded.

So far, the control element has controlled particular modes of vibration. The controller could concentrate on that single mode, and the efficiency was fairly good. If the exciting force is not tuned at the resonances of the plate, which is a more general case, the sensor/actuator pair has to control all the induced modes simultaneously, and the efficiency would deteriorate. Figures 13 and 14 show the uncontrolled and controlled vibration amplitude of the plate when the point load is applied at 30 radians/sec while (1, 1) resonance frequency is 120 radians/sec. Maximum reduction is -43.4 dB and average reduction is -6.1 dB. The results confirm the above argument. Use of more control elements, each one aimed at specific modes, will improve the efficiency. In conclusion, these results verify the effectiveness of the Eq. 29.

4.1.2 multiple point load and one PZT sensor/ actuator pair

Equation 29 is a general equation accommodating arbirtary number of loads and sensor/actuator pairs. To check the validity of the equation for multiple number of external forces, three point loads are applied to the plate and one PZT sensor/actuator pair is used to control the vibration. External loads are located at (0.09, 0.27), (0.27, 0.09), (0.27, 0.27) and the sensor/actuator pair at (0.18, 0.18). Magnitude of each load is lowered down to 2 N to prevent unrealistic vibration. Source frequency tuned at the first resonance of the plate produces the amplitude response almost the same as Fig. 3. Figure 15 shows the vibration amplitude when the control effect is included. Effect of nearby two point loads is cancelled a lot, but that of the farther load at (0.27, 0.27) is still pronounced. Amplitude peak decreases from 4 cm to 0.8 cm. Maximum suppression occurs around the actuator and is 64.4 dB. Average reduction is 31.4 dB. For higher modes, similar results are obtained, and they are summarized in Table 2. Comparison of the two sets of data in Table 2 does not show much differece. That is because, even though the number of the point loads increases, all of them are tuned at a certain frequency. The generated vibration mode does not have much distinct from that of a single point load. The increase of external loads requires more control effort, and it is taken care of by the control unit. In general, average control efficiency decreases with the number and distribution of the loads.

Table 2. Comparison of average vibration amplitude reduction ratio

mode	one point load one sensor/actuator pair	three point load one sensor/actuator pair
1, 1	-24.7	−31.4
1, 2	−23.1	-22.2
2, 2	−28.1	−24.2
1, 3	−15.1	−14.1

unit : dB

4.1.3. one point load and multiple PZT sensor/ actuator pairs

This section investigates the case where the external point load is single, and the PZT sensor/actuator pair is multiple. When 10 N point load is adjusted at the first resonance, the vibration amplitude without control is the same as Fig. 3. With the three actuators turned on, the response diminishes to Fig.16. Due to the increase of control forces, there is a great reduction in the amplitude. Maximum suppression is achieved around the load position as shown in Fig. 17 Results for higher modes consideration are summarized in Table 3.

The case of multiple external forces and mul-

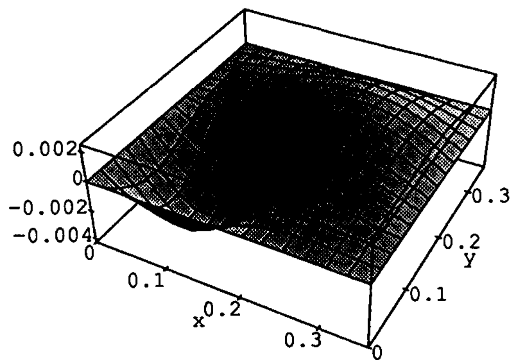

Fig 15. Vibration amplitude response of the simply supported plate exposed to three point loads tuned at (1,1) mode and one **PZT** sensor /actuator pair

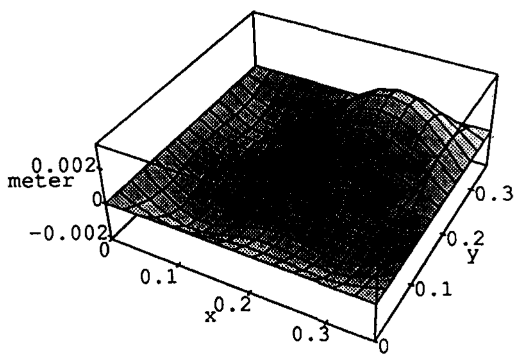

Fig 16. Vibration amplitude response of the simply supported plate exposed to one point load tuned at(1,1) mode and three **PZT** sensor /actuator pairs

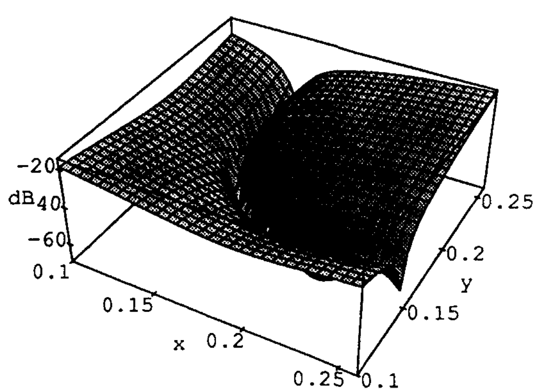

Fig 17. Vibration amplitude reduction after the active vibration control when the plate is exposed to one point load tuned at(1.1) mode

tiple control elements will be treated in Sec. 4.3

Table 3. Comparison of average viration amplitude reduction ratio

mode	one point load one sensor /actuator pair	one point load three sensor /actuator pairs
1, 1	−24.7	−30.5
1, 2	−23.1	−24.2
2, 2	−28.1	−29.1
1, 3	−15.1	−17.1

unit : dB

4.2. Piezoelectric Drivers

Instead of the point load, the external load is given by a small **PZT** planar driver. The driver is basically the same as the actuator. Just the role of the element is different. When the plate is driven by the driver, the initial force is given in the form of bending moment like

$$m_{dxj} = m_{dyj} = Y_d \, d_{31}(t_d + t_p) \, V_d = m_{dj}. \tag{34}$$

where V_d is driver electric voltage, t_d the thickness, and Y_d the effective Young's modulus of the driver, respectively. When the dimension of the piezoelectric driver is considered, the initial bending moment is given as

$$\begin{aligned} M_{dxj} &= m_{dj}[h(x-x_{dj1}) - h(x-x_{dj2})] \\ &\quad [h(y-y_{dj1}) - h(y-y_{dj2})], \\ M_{dyj} &= m_{dj}[h(x-x_{dj1}) - h(x-x_{dj2})] \\ &\quad [h(y-y_{dj1}) - h(y-y_{dj2})]. \end{aligned} \tag{35}$$

These moments replace the forcing term $F(x_d, y_d)$in Eq. 12 as

$$D\nabla^4 w + \rho\ddot{w} = \frac{\partial^2 M_{dxj}}{\partial x^2} + \frac{\partial^2 M_{dyj}}{\partial y^2} \tag{36}$$

In the same manner as before, with Eq. 18, the coefficient α'_{mn} is determined as

$$\alpha'_{mn} = \frac{4m_{dj}}{\rho\, ab(\omega_{mn}^2 - \omega^2)} \left(\frac{\frac{(m\pi)^2}{a} + \frac{(n\pi)^2}{b}}{\frac{m\pi}{a} \; \frac{n\pi}{b}} \right)$$

$$\left[\cos\left(\frac{m\pi x_{dj1}}{a}\right) - \cos\left(\frac{m\pi x_{dj2}}{a}\right)\right]$$

$$\left[\cos\left(\frac{m\pi y_{d1}}{b}\right) - \cos\left(\frac{m\pi y_{d2}}{b}\right)\right] \tag{37}$$

The only difference between the point load and the **PZT** driver is the way of providing initial load to the plate. Point load is giving a direct force term as the $P(x_d, y_d)$ in Eq. 12. and the **PZT** driver is giving a moment term. Generated vibration of the plate should not change with respect to the way of receiving energy. In addition, the point load operates on just a single point. But the **PZT** driver operates on a planar area of the driver size even if small. This operation area can cause some difference in the control effort and the generation of higher modes of vibration. For the various arrangement of number and location of the drivers and controllers, however, results should be basically almost the same as those in Sec. 4.1. as long as the driver is not large. If we look at the case of one 1cm × 1cm **PZT** driver and one **PZT** sensor/actuator pair, the amplitude response shape is the same as Fig. 3 and 4. Amplitude reduction ratio in Fig. 18 changes a little bit from that of Fig. 6 and this difference reflects the effect of exciter type change. Control results for the four modes are summarized in Table 4.

Table 4. Comparison of average vibration amplitude reduction ratio

mode	one point load one sensor/actuator pair	one **PZT** driver one sensor/actuator pair
1, 1	−24.7	−24.4
1, 2	−23.1	−23.3
2, 2	−28.1	−29.0
1, 3	−15.1	−16.1

unit : dB

Point Loads and Piezoelectric Drivers

Both point and **PZT** drivers are used as the initial external load source, and multiple pairs of **PZT** sensor/actuator are used as the control

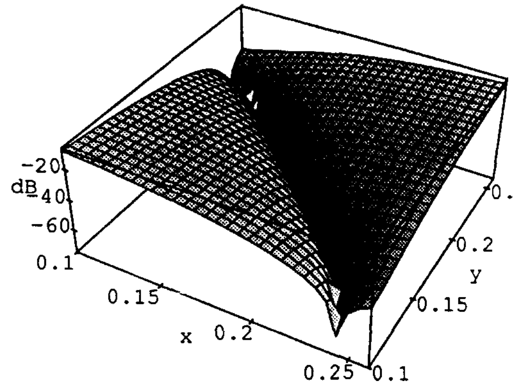

Fig 18. Vibration amplitude reduction after the active vibration control when the plate is exposed to one **PZT** driver tuned at(1,1) mode

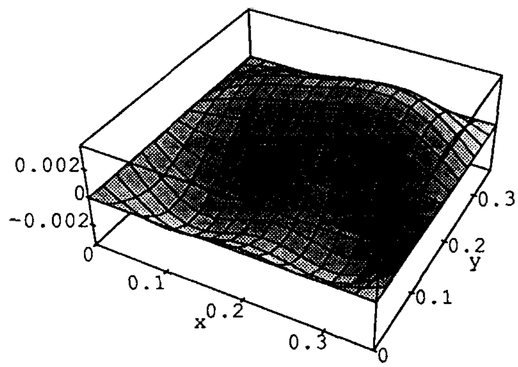

Fig 19. Vibration amplitude response of the simply supported plate exposed to one point load and one **PZT** driver, both tuned at(1,1) mode, as well as two **PZT** sensor/actuator pairs

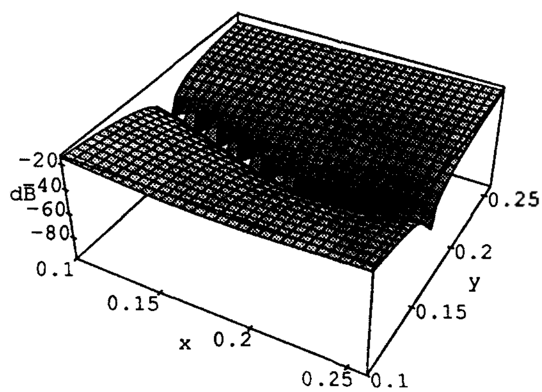

Fig 20. Vibration amplitude reduction after the active vibration control when the plate is exposed to one point load and one **PZT** driver, both tuned at(1, 1) mode

elements. This corresponds to the case of multiple external forces and multiple control elements. One 10 N point load is placed at(0.27, 27), the center of one 20 Nm **PZT** driver at(0.09, 0.27), and the centers of two **PZT** sensor/actuator pairs at(0.09, 0.09) and (0.27, 0.09), respectively. When both of the vibration sources are tuned at the first resonance of the plate, amplitude response without the control effect is almost the same as Fig. 3. Figure 19 shows the response with the actuator on. Amplitude reduction ratio is described in Fig. 20. The figure clearly shows the external force dominating zone and the control moment dominating zone. Maximum amplitude suppression occurs around the actuator and is −90 dB. Average suppression is −26.4 dB. Further results are summarized in Table 5.

These prove the validity of the Eq. 29 for multiple input forces and multiple pairs of the piezoelectric sensor/actuator.

Table 5. Comparison of average vibration amplitude reduction ratio

mode	one point load one sensor/actuator pair	one point load, one PZT driver two sensor/actuator pair
1, 1	−24.7	−26.4
1, 2	−23.1	−25.4
2, 2	−28.1	−23.5
1, 3	−15.1	−15.4

unit : dB

V. Conclusion

Theoretical aspects of active vibration control of a simply supported plate were investigated using piezoelectric sensors and actuators. Appropriate dynamic equations of the piezoelectric sensor and actuator for the control purpose were derived and coupled with the governing equation of the plate. Analytic solution of the modified equation of motion allows detailed analysis of the vibration amplitude response of the plate to the combined effect of external driving forces and piezoelectric control moments. To illustrate the solution, numerical analysis was performed with concentrated point loads and **PZT** plate drivers. The results demonstrate the effectiveness of the solution as well as the piezoelectric sensors and actuators. The approach investigated in this work can be applied to arbitrary external loading conditions and control algorithm. Experimental verification of the theoretical results will be presented next.

References

1. Proceedings of international symposium on active control of sound and vibration, Acoustical Society of Japan, Tokyo, Japan, May, 1991
2. J.L.Fanson and T.K.Caughey, "Positive position feedback control for large space structures", AIAA paper 87-0902, 1987
3. M.J.Balas, "Modal control of certain flexible dynamic systems", SIAM Journal of Control and Optimization, vol. 16, No. 3, pp.450-462, 1978
4. D.B.Schaechter, "Optimal local control of flexurable structures," Journal of Guidance and Control, vol. 4, No. 1, pp. 22-26, 1981
5. T.Bailey and J.E.Hubbard, "Distributed piezoelectric polymer active vibration control of a cantilever beam," Journal of Guidance and Control, vol. 8, No 8, pp. 605-611, 1985
6. B.A.Auld, Acoustic fields and waves in solids, vol. 1, John Wiley & Sons, New York, 1973
7. J.F.Nye, Physical properties of crystals, Oxford University Press, New York, 1985
8. Y.R.Roh, "Active vibration control with piezoelectric sensors and actuators," Proceedings of Kores-Japan joint symposium on acoustics, pp. 403-408, 1991
9. S.Timoshenko and S.Wonowsky-Krieger, Theory of plates and shells, McGraw Hill, New York, 1970
10. J.A.Nelder and R.Mead, "A simplex method for function minimization", Computer Journal, vol. 7, pp. 308−312, 1965

Yongrae Roh received the B. S. and M. S. degrees in Mineral and Petroleum Engineering from the Seoul National University, Seoul in 1984 and 1986, respectively. He got the Ph. D. degree in Engineering Science and Mechanics(major in Acoustics) from the Pennsylvania State University, U. S. A., in 1990. He is currently a senior research scientist in the Research Institute of Industrial Science & Technology, Pohang. Major research area includes SAW devices, ultrasonic transdcers, and noise & vibration control. He received the 1990 Xerox Award, U.S.A., for the best research in mater ials.